

Inhibition of severe acute respiratory syndrome-associated coronavirus (SARS-CoV) infectivity by peptides analogous to the viral spike protein

Bruno Sainz Jr.^{a,*}, Eric C. Mossel^{b,1}, William R. Gallaher^c, William C. Wimley^d,
C.J. Peters^{b,e}, Russell B. Wilson^f, Robert F. Garry^a

^a Department of Microbiology and Immunology, Tulane University Health Sciences Center, New Orleans, LA 70112, USA

^b Department of Microbiology and Immunology, University of Texas Medical Branch, Galveston, TX 77555, USA

^c Department of Microbiology, Immunology and Parasitology, Louisiana State University Health Sciences Center, New Orleans, LA 70112, USA

^d Department of Biochemistry, Tulane University Health Sciences Center, New Orleans, LA 70112, USA

^e Department of Pathology, University of Texas Medical Branch, Galveston, TX 77555, USA

^f Autoimmune Technologies, LLC, New Orleans, LA 70112, USA

Received 20 July 2005; received in revised form 9 February 2006; accepted 1 March 2006

Available online 17 April 2006

Abstract

Severe acute respiratory syndrome-associated coronavirus (SARS-CoV) is the cause of an atypical pneumonia that affected Asia, North America and Europe in 2002–2003. The viral spike (S) glycoprotein is responsible for mediating receptor binding and membrane fusion. Recent studies have proposed that the carboxyl terminal portion (S2 subunit) of the S protein is a class I viral fusion protein. The Wimley and White interfacial hydrophobicity scale was used to identify regions within the CoV S2 subunit that may preferentially associate with lipid membranes with the premise that peptides analogous to these regions may function as inhibitors of viral infectivity. Five regions of high interfacial hydrophobicity spanning the length of the S2 subunit of SARS-CoV and murine hepatitis virus (MHV) were identified. Peptides analogous to regions of the N-terminus or the pre-transmembrane domain of the S2 subunit inhibited SARS-CoV plaque formation by 40–70% at concentrations of 15–30 μ M. Interestingly, peptides analogous to the SARS-CoV or MHV loop region inhibited viral plaque formation by >80% at similar concentrations. The observed effects were dose-dependent (IC₅₀ values of 2–4 μ M) and not a result of peptide-mediated cell cytotoxicity. The antiviral activity of the CoV peptides tested provides an attractive basis for the development of new fusion peptide inhibitors corresponding to regions outside the fusion protein heptad repeat regions.

© 2006 Elsevier B.V. All rights reserved.

Keywords: Severe acute respiratory syndrome-associated coronavirus; Class I viral fusion protein; Peptide inhibitor; Murine hepatitis virus; Six-helix bundle; Anti-viral

1. Introduction

Severe acute respiratory syndrome (SARS) is an atypical pneumonia characterized by influenza-like symptoms including fever, cough, dyspnea and headache. The epidemic of 2002–2003 produced an overall mortality of approximately 10%, resulting in 774 deaths in 29 countries world-wide

(Goldsmith et al., 2004; Holmes, 2005; Peiris et al., 2003b). The etiological agent of SARS (SARS-CoV) was quickly identified as belonging to the family *Coronaviridae*, a group of large enveloped RNA viruses exhibiting a broad host range and capable of causing respiratory, hepatic and enteric diseases (Lai and Holmes, 2001; Siddell, 1995). Initial phylogenetic analyses and sequence comparisons revealed significant differences between SARS-CoV and other CoVs, distinguishing it as a unique group (group 4), unrelated to previously characterized CoV groups 1–3 (Drosten et al., 2003; Ksiazek et al., 2003; Peiris et al., 2003a). More recent analyses, however, report that SARS-CoV more closely resembles group 2 CoV and should therefore be classified as a subgroup within group 2 (Gorbalenya et al., 2004; Magiorkinis et al., 2004; Song et al., 2005). Further phylogenetic

* Corresponding author at: The Scripps Research Institute, Molecular and Experimental Medicine, 10550 N. Torrey Pines Rd, SBR-10, La Jolla, CA 92037, USA. Tel.: +1 858 784 2051; fax: +1 858 784 2960.

E-mail address: bsainz@scripps.edu (B. Sainz Jr.).

¹ Present address: Department of Microbiology, Immunology, and Pathology, Colorado State University, Fort Collins, CO 80523-1619, USA.

analyses and studies investigating the ancestral origins of SARS-CoV should yield a consensus regarding its proper grouping. Nonetheless, as animal reservoirs of SARS-CoV appear to exist, reemergence of this unique CoV is highly probable and therefore the threat of a new SARS outbreak remains a constant public health concern.

Like other enveloped viruses, CoVs enter target cells by inducing fusion between the viral and cellular membranes, a process mediated by the viral spike (S) glycoprotein (Gallagher and Buchmeier, 2001). The S1 subunit of the S protein mediates receptor binding (Cavanagh and Davis, 1986; Taguchi, 1995), while the S2 subunit is responsible for driving viral and target cell membrane fusion (Taguchi and Shimazaki, 2000). In the case of SARS-CoV, the S1 subunit binds to the mammalian receptor angiotensin-converting enzyme 2 (ACE2) (Huang et al., 2006; Li et al., 2003, 2005; Wang et al., 2004; Wong et al., 2004) and/or CD209L (Jeffers et al., 2004), initiating the entry process via a cathepsin L-dependent pathway (Huang et al., 2006). Analysis of the murine hepatitis virus (MHV) and SARS-CoV S proteins (Li et al., 2005; Xu et al., 2004a,b,c) reveal common structural features shared with class I viral fusion proteins (Gallagher, 1996; Gallagher et al., 1989), including a hydrophobic fusion peptide (Sainz et al., 2005b), a pair of extended α helices (N-helix and C-helix) (Tripet et al., 2004), a loop domain separating the two α helices and a cluster of aromatic amino acids (Sainz et al., 2005a) proximal to a hydrophobic transmembrane anchoring domain. Class I viral fusion proteins mediate viral and target cell membrane fusion through a series of conformational changes involving insertion of a fusion peptide into the target cell membrane, trimerization and extension of the heptad repeat (HR) helices toward the target membrane and the subsequent formation of a six-helix coiled-coil bundle (Gallagher, 1987). In this structure, a trimer of HR1 helices forms a central coiled-coil surrounded by three HR2 helices in an anti-parallel mode (Xu et al., 2004b). The loop region is believed to act as a hinge, facilitating six-helix coiled-coil bundle formation and mediating membrane juxtaposition.

While current models of viral:cell membrane fusion are hypothetical in most aspects, the importance of several of the structural/functional motifs of class I viral fusion proteins as drug development targets has been established. For example, analogs of the orthomyxovirus, paramyxovirus (Richardson et al., 1980) and HIV-1 fusion peptide domains (Gallagher et al., 1992; Owens et al., 1990; Silburn et al., 1998) block viral infection, presumably by forming inactive heteroaggregates. Likewise, peptides analogous to the HR regions of the HIV-1 (Gallagher et al., 1992; Qureshi et al., 1990; Wild et al., 1992, 1993), paramyxovirus (Lambert et al., 1996; Young et al., 1999) or Ebola virus (EboV) (Watanabe et al., 2000) class I viral fusion proteins block virion infectivity by preventing the transition of the fusion protein into the six-helix bundle state. The anti-HIV-1 peptidic drug FuzeonTM (DP178, T-20 or enfuvirtide), which overlaps HR2 and the aromatic domain of gp41, was the first of a new class of fusion inhibitor antivirals to gain FDA approval (2003). This peptide has been shown to potently inhibit HIV-1 virion:cell fusion at very low concentrations (50% inhibition at 1.7 nM) in vitro (Wild et al., 1993). Likewise, in clinical trials, 100 mg/day

of FuzeonTM caused an \sim 100-fold reduction in plasma HIV-1 load of infected individuals (Kilby et al., 1998; Lalezari et al., 2003a,b). These results substantially validate the efficacy of this new class of antivirals and have greatly motivated the search for peptide fusion inhibitors designed to target other viruses, such as SARS-CoV (Gallagher and Garry, 2003; Klinger and Levanon, 2003).

To date, studies examining peptide fusion inhibitors of CoV have only examined the efficacy of peptides analogous to the HR regions of the viral fusion protein. Bosch et al. (2003) first demonstrated that a peptide analogous to the HR2 helix of the MHV S2 subunit could block viral entry at concentrations of 10–50 μ M. Several other groups later showed that HR1 and/or HR2 peptides could likewise inhibit SARS-CoV entry and replication (Bosch et al., 2004; Liu et al., 2004; Yuan et al., 2004; Zhu et al., 2004). The antiviral capacity of these peptides is attributed to the inherent interactions between HR1 and HR2 (Tripet et al., 2004; Xu et al., 2004b,c). Peptides analogous to either one of the two HR regions are believed to directly inhibit endogenous HR1 and HR2 interactions, preventing formation of the six-helix bundle.

Although the HR analogs appear to be effective inhibitors of SARS-CoV entry in vitro, development of other peptide fusion inhibitors, based on non-HR regions of the viral fusion protein, has yet to be explored. Here we employed a novel approach to identify new peptide inhibitors of SARS-CoV. Using the Wimley and White (WW) interfacial hydrophobicity scale (IHS) (Wimley and White, 1996), we identified five regions within the SARS-CoV and MHV S2 subunit with a high propensity to interact with the lipid interface of membranes. These regions, spanning the entire S2 subunit, may play an important role in viral fusion protein:target cell membrane interactions and may therefore represent possible targets for therapeutic interference. Our results demonstrate that peptides analogous to these regions of high interfacial hydrophobicity are effective inhibitors of SARS-CoV infectivity. In particular, peptides analogous to the loop region and/or the N-terminal region of the S2 subunit potently inhibit CoV plaque formation by 70–90% at concentrations of 30 μ M or less (\sim 100 μ g/ml). These findings provide an alternative approach to the development of viral peptide inhibitors, allowing for the identification of other possible therapeutic peptides outside of the HR regions of class I viral fusion proteins.

2. Materials and methods

2.1. Peptide synthesis

The MHV and SARS-CoV synthetic peptides were synthesized by solid-phase methodology using a semi-automated peptide synthesizer and conventional N-alpha-9-fluorenylmethoxycarbonyl chemistry by Genemed Synthesis Inc. (San Francisco, CA). Peptides were purified by reversed-phase high performance liquid chromatography, and their purity confirmed by amino acid analysis and electrospray mass spectrometry. Peptide stock solutions were prepared in 10% dimethyl sulfoxide (DMSO, spectroscopy grade): 90%

H₂O (v/v), and concentrations determined spectroscopically (SmartSpec™ 3000, BioRad, Hercules, CA).

2.2. Cells and viruses

Vero E6 and L2 cells (American Type Culture Collection, Manassas, VA) were maintained in minimum essential medium (MEM) or Dulbecco modified Eagle medium (DMEM), respectively, and supplemented with 5% fetal bovine serum (FBS), penicillin G (100 U/ml), streptomycin (100 mg/ml) and 2 mM L-glutamine, at 37 °C in 5% CO₂. SARS-CoV strain Urbani was propagated in Vero E6 cells, and MHV strain A59 (ATCC, VR764) was propagated in L2 cells.

2.3. Viral plaque reduction assays

For plaque reduction assays, Vero E6 cells or L2 cells were seeded at a density of 1×10^6 cells in each well of a 6-well plate 24 h (h) prior to infection. Approximately 50 plaque forming units (PFU) of either SARS-CoV strain Urbani or MHV were pre-incubated with peptide or without peptide (diluent control) in serum-free MEM (SARS-CoV) or serum-free DMEM (MHV) for 1 h at 37 °C. Vero E6 or L2 cells were then infected with (1) peptide- or vehicle-treated SARS-CoV inoculum or (2) peptide- or vehicle-treated MHV inoculum, respectively. After 1 h adsorption, the inoculum was removed, cells were washed twice with $1 \times$ phosphate buffered saline (PBS), and then overlaid with 10% FBS/MEM or 10% FBS/DMEM, both containing 0.5% Noble Agar (Sigma, Rockland, ME). L2 cells were fixed 2 days p.i. with 3.7% formalin for 2 h at room temperature and then stained with $1 \times$ crystal violet to visualize plaques. Vero E6 cells were stained with neutral red 3 days p.i. and plaque numbers were determined 24 h later.

2.4. Cell viability assay

Cell viability was determined by using the TACS™ MTT Assay (R&D Systems Inc., Minneapolis, CA) according to the manufacturer's instructions. Briefly, Vero E6 cells or L2 cells were seeded at a density of 4×10^5 cells in each well of a 96-well plate 24 h prior to treatment. Cells were subsequently treated with medium, diluent-control or 100 μg/ml (~30 μM) of peptide for 2 h prior to the addition of the tetrazolium compound MTT. Following incubation and subsequent addition of detergent, absorbance was read at 570 nm with a spectrophotometer.

2.5. CD spectroscopy

CD spectra were recorded on a Jasco J-810 spectropolarimeter (Jasco Inc., Easton, MD), using a 1 mm path length, 1 nm bandwidth, 16 s response time and a scan speed of 10 nm/min. All CD runs were performed at room temperature with 50 μM peptide dissolved in 10 mM phosphate (PO₄) buffer at pH 7.0. Three successive scans between 190 and 250 nm were collected and the CD data are expressed as the mean residue ellipticity, derived from the formula $\Theta = (\text{deg} \times \text{cm}^2)/\text{dmol}$.

2.6. Proteomics computational methods

Methods to derive general models of surface glycoproteins have been described previously (Gallaher et al., 1989). Domains with high interfacial hydrophobicity were identified with Membrane Protein eXplorer (MPeX; Stephen White laboratory; <http://blanco.biomol.uci.edu/mpex>). MPeX detection of membrane spanning sequences is based on experimentally determined hydrophobicity scales (White and Wimley, 1999; Wimley and White, 1996).

2.7. Statistics

Data are presented as the mean \pm standard error of the means (S.E.M.). Data from peptide-treated groups were compared to vehicle-treated groups and significant difference were determined by one-way analysis of variance (ANOVA) followed by Tukey's post hoc *t*-test (GraphPad Prism©, San Diego, CA).

3. Results

3.1. Identification of peptides analogous to the CoV S2 subunit

Previous studies of potential peptide inhibitors of CoV have only examined the efficacy of peptides corresponding to the α helical regions (HR regions) of the S2 subunit (Bosch et al., 2004; Liu et al., 2004; Yuan et al., 2004; Zhu et al., 2004). Development of additional peptide fusion inhibitors, based on domains of the viral fusion protein other than the prominent α helices, has yet to be explored. We used a computational approach to identify regions of the SARS-CoV fusion protein that potentially interact with bilayer membranes (Wimley and White, 1996). The WWIHS is an experimentally-determined algorithm that can be used to estimate the propensity of an amino acid sequence to interact with the lipid membrane interface (Wimley and White, 1996). Five regions of high interfacial hydrophobicity within the SARS-CoV S2 region were identified using Membrane Protein eXplorer (MpeX) (<http://blanco.biomol.uci.edu/mpex/>), a computer program based on the WWIHS (Fig. 1A). WW-I and WW-II peptides correspond to the amino-terminus of the S2 region, predicted to contain the fusion peptide (Sainz et al., 2005b). WW-III and WW-IV peptides correspond to the loop domain and the WW-V peptide corresponds to the aromatic domain. The latter is a highly conserved region among the *Coronaviridae* family and is also present in class I viral fusion proteins of otherwise disparate RNA viruses, such as HIV-1 and EboV (Sainz et al., 2005a). The transmembrane domain of the S2 region also scored high on the WWIHS (Fig. 1A), but was not investigated as it is anchored within the viral membrane and not exposed during viral entry. Although the SARS-CoV S protein shares only 20–27% amino acid sequence similarity with the S protein of MHV (Rota et al., 2003), five analogously located sequences of high interfacial hydrophobicity were identified in the S2 subunit of MHV strain A59 (Fig. 1B) and strain BHK (data not shown).

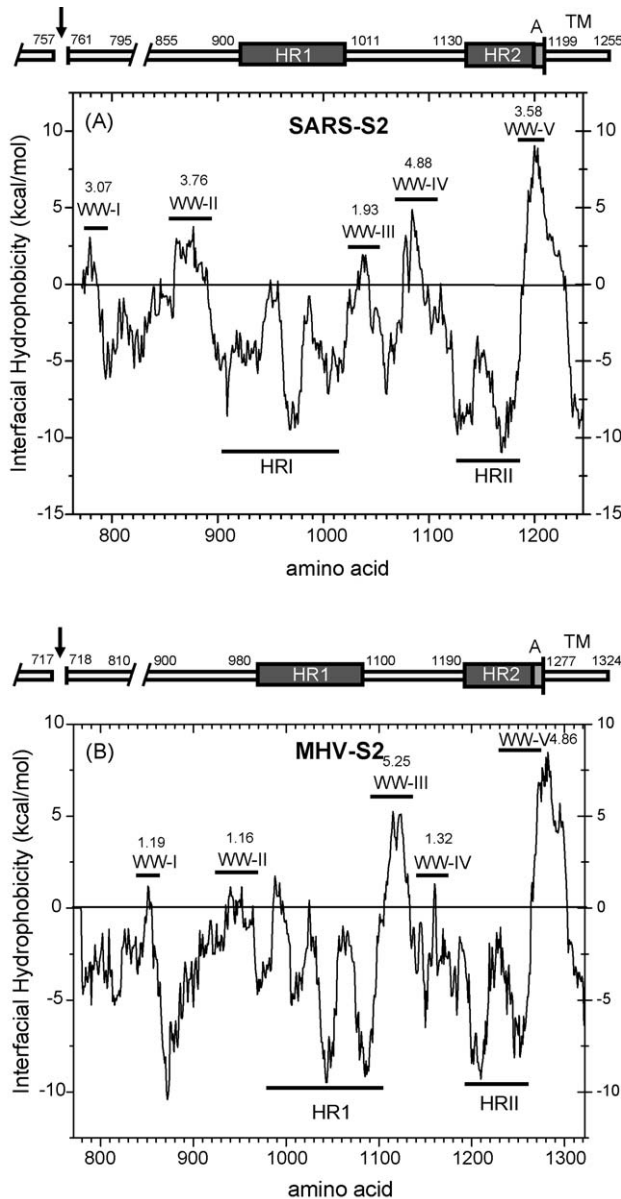


Fig. 1. (A) Interfacial hydrophobicity plot corresponding to sequences of the SARS-CoV strain Urbani S2 subunit (amino acids 758–1255). (B) Interfacial hydrophobicity plot corresponding to sequences of the MHV strain A59 S2 subunit (amino acids 780–1324). Interfacial hydrophobicity plot (mean values for a window of 19 residues) was generated using the WWIHS for individual residues (Wimley and White, 1996). The regions corresponding to areas of high interfacial hydrophobicity identified in both the SARS-CoV and MHV CoV S2 subunits are highlighted by black bars, labeled as WW-I–WW-V, and hydrophobicity scores (kcal/mol) are indicated above. Schematic diagram of the CoV S protein is depicted above each hydrophobicity plot, illustrating the respective domains. HR: heptad repeat, A: aromatic domain, TM: transmembrane domain. The arrows indicates the location of the minimum furin cleavage sites (Molloy et al., 1992) present in the S proteins of SARS-CoV (RNTR, residues 758–761) (Bergeron et al., 2005) and MHV (RRAHRSVS, residues 713–720) (Luytjes et al., 1987).

3.2. Identification of peptide inhibitors of CoV infectivity

Synthetic peptides corresponding to the sequences with significant WWIHS scores were synthesized (Table 1) and exam-

Table 1

Amino acid sequences of peptides corresponding to sequences of the S2 subunits of SARS-CoV or MHV with significant WWIHS scores

Peptide ^a	Amino acid sequence	Net charge	Description	Position
SARS _{WW-I}	<u>M</u> WKTPTLK <u>Y</u> FGG-FNFSQIL ^b	+2	N-terminal	770–788
SARS _{WW-II}	ATAGWTFGAGAAL-	0	N-terminal	864–886
SARS _{WW-III}	QIPFAMQMAY GYHLMSPQAAP- HG ^u VVFLHVTW	+3	Loop	1028–1049
SARS _{WW-IV}	G ^u VFVNGTSW- FITQRNFFS	+1	Loop	1075–1093
SARS _{WW-Va}	NEVAKNLNES- LIDLQELGKYE- QYIKWPWYVW	-2	HR2- Aromatic	1169–1199
SARS _{WW-Vb}	AACEVAKNLNES- LIDLQELGKYE- QYIKW	-2	HR2- Δ Aromatic	1169–1194
MHV _{WW-III}	GNHILSLVQNAP- YGLYFIHFSW	+2	Loop	1096–1117
MHV _{WW-IV}	GYFVQDDGE- WKFTGSSYYY	-3	Loop	1144–1162

^a The SARS-CoV (SARS_{WW}) and MHV (MHV_{WW}) peptides were synthesized based on the amino acid sequence determined from GenBank accession no. AY278741 (SARS-CoV strain Urbani) or AY700211 (MHV strain A59).

^b Amino acid change to tryptophan (W) is shown in underlined text.

ined for their ability to inhibit either SARS-CoV plaque formation on Vero E6 cells, at peptide concentrations of $\sim 30 \mu\text{M}$ (Fig. 2). SARS_{WW-I} and SARS_{WW-II} inhibited viral plaque formation by 58 and 39%, respectively. SARS_{WW-Va}, however, did not show any inhibitory effect at this concentration. This peptide was of particular interest as it was modeled after the HIV-1 peptide inhibitor, FuzeonTM (Kilby et al., 1998) and corresponds to the C-terminus of the C-helix and the aromatic domain. Previous work from our laboratory has shown that the aromatic domain of both the SARS-CoV and MHV S2 subunit partition into the membranes of lipid vesicles and are capable of compromising membrane integrity (Sainz et al., 2005a). We hypothesized that the inability of SARS_{WW-Va} to inhibit SARS-CoV entry may be due to its propensity to partition into the lipid interface (Sainz et al., 2005a). A WW-V derivative with a five amino acid truncation of the aromatic domain (SARS_{WW-Vb}, Table 1) was capable of inhibiting SARS-CoV plaque formation by 42% (Fig. 2A). Peptides corresponding to the loop region of the SARS-CoV fusion protein were the most effective at inhibiting SARS-CoV plaque formation. SARS_{WW-III} and SARS_{WW-IV} inhibited viral plaque formation by 90 and 83%, respectively (Fig. 2A). Shown in Fig. 2B–D is a representative photograph of SARS-CoV plaque formation in the presence of these two peptides. Consistent with the experimental results presented in Fig. 2A, SARS-CoV plaque efficiency was significantly inhibited in the presence of SARS_{WW-III} and SARS_{WW-IV}, as compared to vehicle-treated controls (Fig. 2C–D versus B).

To confirm that the observed anti-viral activity of the peptides tested was not a consequence of cellular cytotoxicity, a

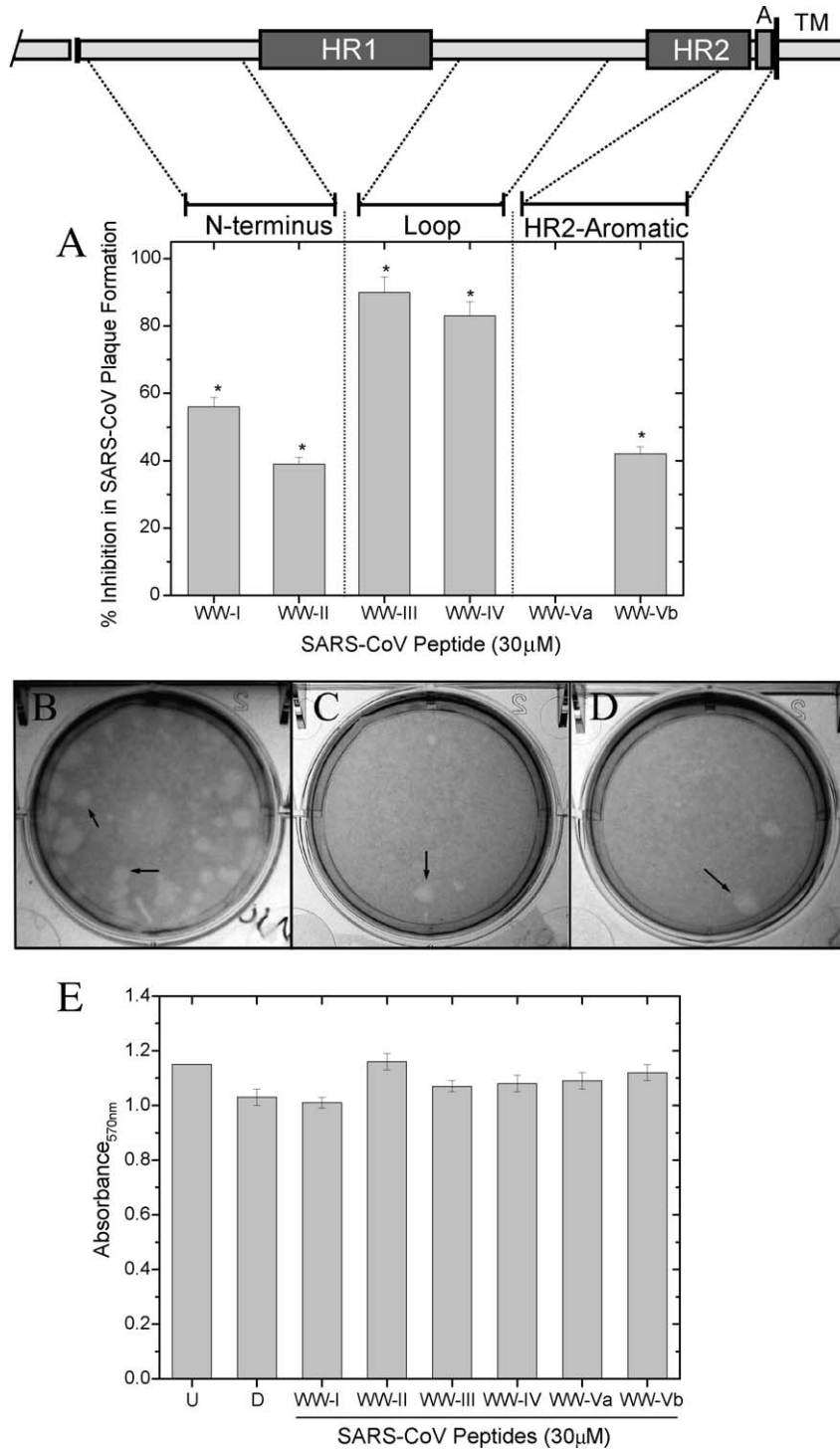


Fig. 2. Effect of peptides analogous to the viral S protein on SARS-CoV plaque formation. (A) Vero E6 were infected with virus pre-incubated for 1 h with 30 μM peptide. Cells were subsequently infected for 1 h, overlaid with medium containing 0.5% agarose and 4 days p.i., plaque numbers were determined. Percent inhibition in plaque formation was calculated as: $100 - ((\text{no. plaques in peptide-treated} / \text{no. plaques in vehicle-treated}) \times 100)$. Significant reductions in plaque numbers relative to vehicle-treated cultures are denoted by a single asterisk ($p < 0.05$, one-way ANOVA and Tukey's post hoc t -test). Vero E6 cells were infected with ~40 PFU of SARS-CoV strain Urbani following a 1 h incubation with (B) vehicle or 30 μM of (C) SARS_{WW-III} or (D) SARS_{WW-IV}. Cells were stained with neutral red 3 days p.i., and cultures were photographed 24 h later. Arrows indicate representative SARS-CoV plaques. (E) SARS-CoV peptides do not affect cell viability. Vero E6 cells were treated for 2 h with 30 μM of SARS-CoV peptides. Cell viability was measured using the TACS™ MTT assay, and absorbance (OD₅₇₀) is plotted for untreated (U), diluent-treated (D) and peptide-treated cultures.

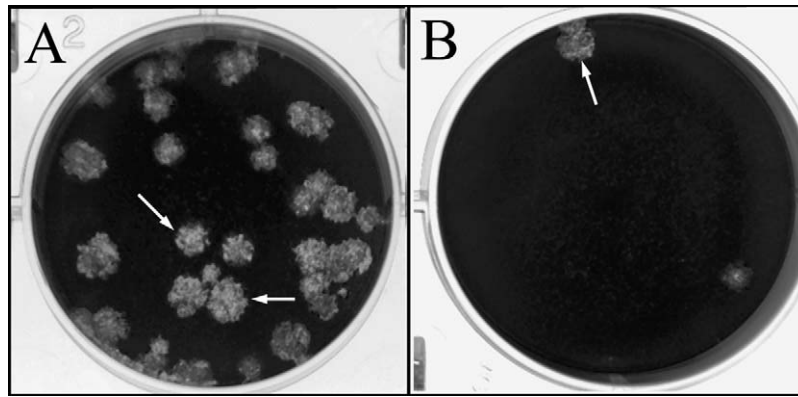


Fig. 3. Peptides analogous to the loop region of the MHV S2 subunit inhibit viral plaque formation. L2 cells were infected with ~ 40 PFU of MHV-A59 following a 1 h incubation with (A) vehicle or $30 \mu\text{M}$ of (B) $\text{MHV}_{\text{WW-IV}}$. Cells were fixed and stained with crystal violet 2 days p.i., and cultures were photographed 24 h later. Arrows indicate representative MHV plaques.

MTT assay was performed as described in Section 2.4. Cells were treated with the tetrazolium compound MTT, which is reduced by metabolically active viable cells to purple formazan dye crystals. Absorbance (OD_{570}) of solubilized crystals in peptide-treated or diluent-treated groups can be compared to untreated controls. Vero E6 cells treated with $\sim 30 \mu\text{M}$ of SARS-CoV peptides showed no difference in absorbance as compared to untreated cells. Likewise, diminished cell viability was not observed in cells treated with diluent control (Fig. 2E). These data indicate that the anti-viral capacity of the SARS-CoV peptides is not a result of cell cytotoxicity, which could directly affect CoV plaque formation.

3.3. Peptides analogous to the loop region of the MHV fusion protein inhibit MHV A59 plaque formation

The potent anti-viral effect observed with the SARS-CoV loop peptides prompted us to test whether peptides analogous to regions located within the loop of the MHV fusion protein had similar anti-viral efficacy. As illustrated in Fig. 1B, the MHV fusion protein also contains five regions of high interfacial hydrophobicity as determined by the WWIHS. Similar to the SARS-CoV fusion protein, two of these regions ($\text{MHV}_{\text{WW-III}}$ and $\text{MHV}_{\text{WW-IV}}$) are located within the MHV S2 loop region. Synthetic peptides corresponding to these two regions (Table 1) were synthesized and examined for their ability to inhibit MHV strain A59 plaque formation on L2 cells at peptide concentrations of $\sim 30 \mu\text{M}$. $\text{MHV}_{\text{WW-III}}$ and $\text{MHV}_{\text{WW-IV}}$ inhibited viral plaque formation by 22 and 98%, respectively (data not shown). Unlike the synthetic SARS-CoV loop peptides tested ($\text{SARS}_{\text{WW-III}}$ and $\text{SARS}_{\text{WW-IV}}$), only one of the MHV loop peptides ($\text{MHV}_{\text{WW-IV}}$) significantly inhibited MHV plaque formation on L2 cells. The potent anti-viral activity of $\text{MHV}_{\text{WW-IV}}$ is illustrated in Fig. 3. As compared to vehicle-treated controls, MHV plaque efficiency was significantly inhibited in the presence of $\text{MHV}_{\text{WW-IV}}$ (Fig. 3A versus B). Moreover, similar to the MTT assay results observed with the SARS-CoV peptides, the $\text{MHV}_{\text{WW-IV}}$ peptide was not cytotoxic at a concentration of $30 \mu\text{M}$ on L2 cells (data not shown).

3.4. Peptide-mediated inhibition of CoV plaque formation is dose-dependent

Based on the results presented above, we chose to further examine the inhibitory potential of $\text{SARS}_{\text{WW-III}}$, $\text{SARS}_{\text{WW-IV}}$ and $\text{MHV}_{\text{WW-IV}}$, as these peptides achieved levels of inhibition of greater than 70% at concentrations of $\sim 30 \mu\text{M}$. Dose–response curves were generated for each peptide, where percent inhibition in viral plaque formation was plotted as function of peptide concentration (Fig. 4). The inhibition efficiency of these peptides was maintainable at low concentrations. The 50% inhibitory concentration (IC_{50}) for both $\text{SARS}_{\text{WW-III}}$ and $\text{SARS}_{\text{WW-IV}}$ was approximately $2 \mu\text{M}$ (Fig. 4A and B). The other SARS-CoV peptides were statistically ineffective at concentrations less than $30 \mu\text{M}$ (data not shown). Similarly, the IC_{50} value for $\text{MHV}_{\text{WW-IV}}$ was $4 \mu\text{M}$ (Fig. 4C). In addition, the SARS-CoV loop peptides were ineffective inhibitors of MHV infectivity, suggesting some degree of sequence-specific inhibition (data not shown).

3.5. Circular dichroism analysis of the CoV loop peptide inhibitors

HR peptide inhibitors of SARS-CoV or MHV have α -helical structure and inhibit viral entry through coiled coil interactions (Bosch et al., 2003, 2004; Liu et al., 2004; Zhu et al., 2004). To assess the propensity of the loop peptides studied herein to adopt a defined secondary structure, peptides were examined by CD spectroscopy (Fig. 5). No distinct α -helical (minima at 208 and 222 nm) or β -sheet (minima at ~ 218 nm) spectra were observed for any of the peptides in 10 mM PO_4 buffer pH 7.0. Rather, spectra for all peptides in buffer showed single minima at or near 200 nm indicative of a random coil.

4. Discussion

$\text{SARS}_{\text{WW-I}}$ and $\text{SARS}_{\text{WW-II}}$ have been independently identified as putative fusion peptides of the SARS-CoV S protein using biophysical approaches (Sainz et al., 2005b). Peptides

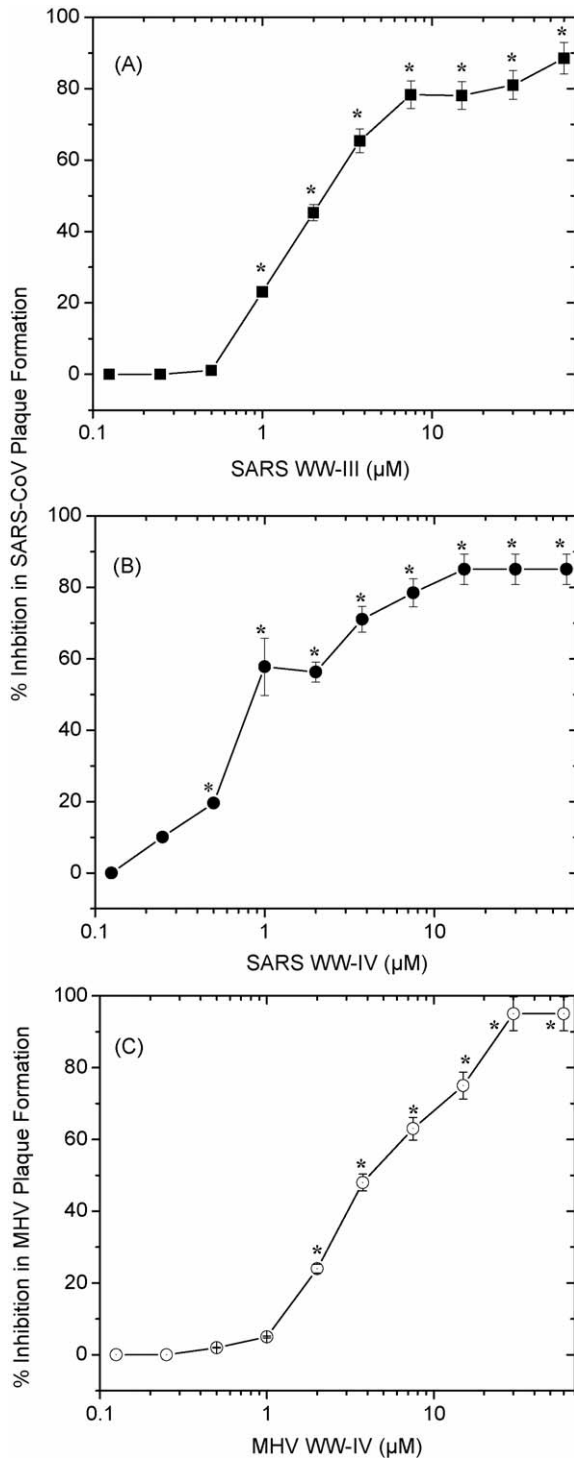


Fig. 4. Peptide-mediated inhibition of CoV plaque formation is dose dependent. Vero E6 cells were infected with SARS-CoV following a 1 h incubation with varying concentrations (0.125–60 μM) of (A) SARS_{WW-III} or (B) SARS_{WW-IV}. L2 cells were infected with MHV-A59 following 1 h incubation with varying concentrations (0.125–60 μM) of (C) MHV_{WW-IV}. Percent inhibition in plaque formation was calculated as: $100 - ((\text{no. plaques in peptide-treated} / \text{no. plaques in vehicle-treated}) \times 100)$. Significant reductions in plaque numbers relative to vehicle-treated cultures are denoted by a single asterisk ($p < 0.05$, one-way ANOVA and Tukey's post hoc t -test).

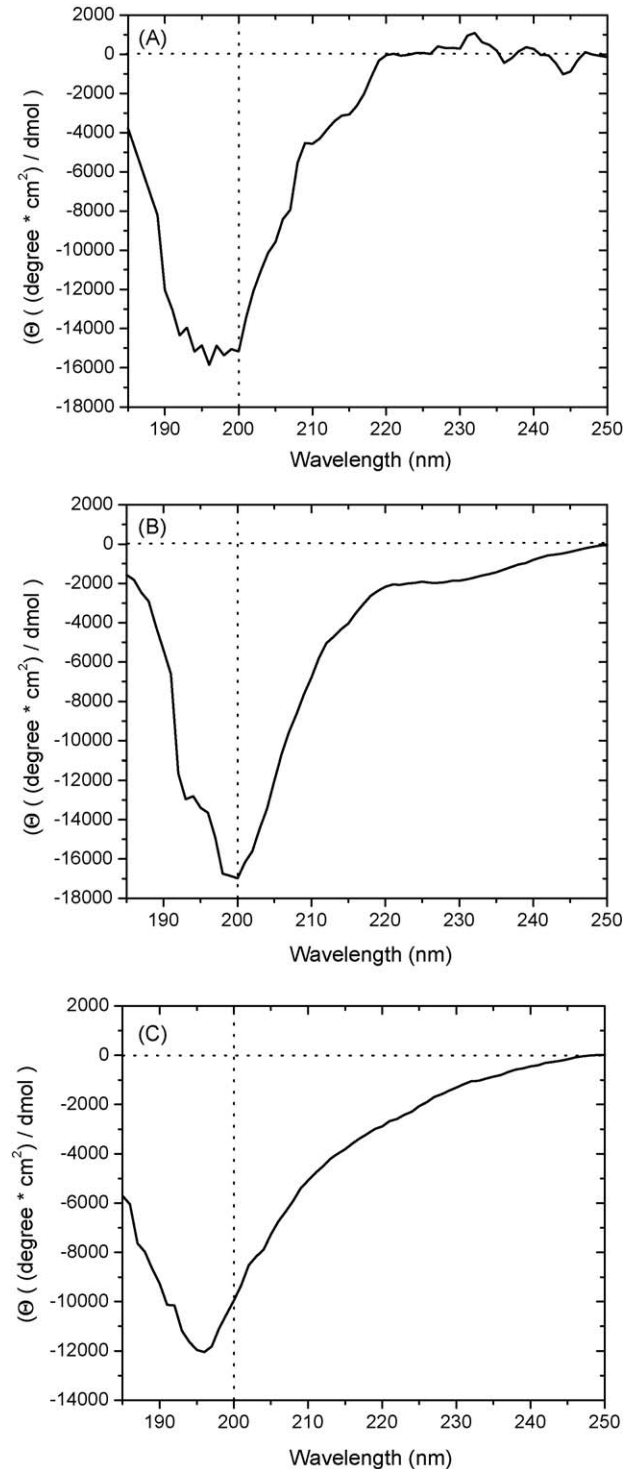


Fig. 5. CoV inhibitory peptides do not assume a defined secondary structure. CD spectra (mean residue ellipticity Θ) of the SARS-CoV peptides: (A) SARS_{WW-III} and (B) SARS_{WW-IV} or the MHV peptide: (C) MHV_{WW-IV} in 10 mM PO_4 buffer pH 7.0 at room temperature.

analogous to class I fusion peptides often have antiviral activity (Gallaher et al., 1992; Owens et al., 1990; Silburn et al., 1998). The observation that WW-I and/or WW-II sequences inhibit infection (Fig. 2A), provides further evidence for their roles in initiating CoV virion:cell fusion; however, it cannot be ruled out that the fusion peptide(s) of SARS-CoV may be in a position different from other class I fusion proteins, e.g. the loop domain (WW-III or WW-IV), and the membrane interactions and conformational changes that CoV S undergoes may not follow the exact same mechanism.

SARS_{WW-III}, SARS_{WW-IV} and MHV_{WW-IV}, which correspond to sequences in the SARS-CoV or MHV loop domain, exhibited antiviral activity greater than the other peptides studied, inhibiting viral plaque formation with IC₅₀ values of 2–4 μM (Figs. 2–4). Compounds that inhibit virus replication with IC₅₀ in the low μM range can be considered promising lead compounds (Liu et al., 2004; Sia et al., 2002). Inhibition of plaque formation is likely to be the most stringent test of a viral inhibitor. Although different methods were used to quantify the antiviral effects, the IC₅₀ concentrations are similar to or lower than peptide inhibitors corresponding to the HR regions of CoV previously identified. For example, the helical inhibitors described by Bosch et al. (2004) and Liu et al. (2004) exhibited IC₅₀ in the range of 10–40 μM. Further studies are required to define the mechanisms by which the non-helical peptides (SARS_{WW-III}, SARS_{WW-IV} and MHV_{WW-IV}) inhibit CoV infection. We hypothesize that these peptides may sterically hinder the loop, preventing either initial extension of the fusion protein, transition to the six-helix bundle state, or interaction of the S2 subunit with the cellular membrane. A recent study by York and Nunberg (2004) indicated that tryptophan residues in the loop domain of HIV-1 TM are critical for its interactions with the surface glycoprotein (SU), and therefore the inhibitory loop peptides may disrupt analogous S1/S2 region interactions. There is also currently conflicting evidence as to whether or not SARS-CoV S undergoes cleavage to S1 and S2 subunits (Bergeron et al., 2005; Wu et al., 2004).

MHV entry is not sensitive to lysosomotropic agents, and most current evidence indicates that MHV enters the cell through direct fusion with the plasma membrane (de Haan et al., 2004). Simmons et al. (2004) reported that inhibitors of endosomal acidification did impair entry of retroviral pseudotype particles bearing SARS-CoV S. Therefore, the peptide inhibitors identified here may block S-mediated membrane fusion at different steps for SARS-CoV and MHV, at the plasma membrane, within endosomal compartments or both. Alternatively, some inhibitory peptides may interact directly with CoV virions. Further studies are required to elucidate the mechanisms by which SARS-CoV and MHV S peptides inhibit infectivity.

The CoV inhibitory loop peptides identified here did not have a propensity to adopt either an α-helical or β-sheet secondary structure, as determined by circular dichroism analysis (Fig. 5). Increasing the secondary structure, for example by the addition of alanine residues to promote α helix formation (Jayasinghe et al., 2001), may increase their antiviral activities. Studies are currently underway to evaluate this hypothesis, and to investigate

other modifications to these CoV inhibitory peptides that may enhance their therapeutic potential.

5. Conclusions

Strategies for the treatment of SARS patients have included broad-spectrum antibiotics, glucocorticoids and ribavirin; however, the efficacy of these treatments is still unclear. Therefore, in order to develop better treatment strategies for future outbreaks, it is imperative to develop new therapeutics. In this study, we provide data to support the further investigation of peptide inhibitors as potential therapeutics for SARS-CoV infection. The immune response to SARS-CoV appears capable, in most individuals, of clearing the infection. Thus, therapeutics that inhibit viral infectivity and reduce SARS-CoV load may extend the window of time during which an effective immune response could arise.

Acknowledgments

This work was supported by the National Institutes of Health (AI054626, AI054238, RR018229, and CA08921; R.F.G.), (GM60000; W.C.W.) and (NO1 AI 25489; C.J.P.). Bruno Sainz is a recipient of a National Research Service Award from the NIAID (AI0543818) and Eric Mossel is a recipient of an Emerging and Re-emerging Diseases Fellowship from the NIAID (AI007536).

References

- Bergeron, E., Vincent, M.J., Wickham, L., Hamelin, J., Basak, A., Nichol, S.T., Chretien, M., Seidah, N.G., 2005. Implication of proprotein convertases in the processing and spread of severe acute respiratory syndrome coronavirus. *Biochem. Biophys. Res. Commun.* 326 (3), 554–563.
- Bosch, B.J., Martina, B.E., Van Der Zee, R., Lepault, J., Haijema, B.J., Versluis, C., Heck, A.J., De Groot, R., Osterhaus, A.D., Rottier, P.J., 2004. Severe acute respiratory syndrome coronavirus (SARS-CoV) infection inhibition using spike protein heptad repeat-derived peptides. *Proc. Natl. Acad. Sci. U.S.A.* 101 (22), 8455–8460.
- Bosch, B.J., van der Zee, R., de Haan, C.A., Rottier, P.J., 2003. The coronavirus spike protein is a class I virus fusion protein: structural and functional characterization of the fusion core complex. *J. Virol.* 77 (16), 8801–8811.
- Cavanagh, D., Davis, P.J., 1986. Coronavirus IBV: removal of spike glycopolyptide S1 by urea abolishes infectivity and haemagglutination but not attachment to cells. *J. Gen. Virol.* 67, 1443–1448.
- de Haan, C.A., Stadler, K., Godeke, G.J., Bosch, B.J., Rottier, P.J., 2004. Cleavage inhibition of the murine coronavirus spike protein by a furin-like enzyme affects cell–cell but not virus–cell fusion. *J. Virol.* 78 (11), 6048–6054.
- Drosten, C., Gunther, S., Preiser, W., van der Werf, S., Brodt, H.R., Becker, S., Rabenau, H., Panning, M., Kolesnikova, L., Fouchier, R.A., Berger, A., Burguere, A.M., Cinatl, J., Eickmann, M., Escriou, N., Grywna, K., Kramme, S., Manuguerra, J.C., Muller, S., Rickerts, V., Sturmer, M., Vieth, S., Klenk, H.D., Osterhaus, A.D., Schmitz, H., Doerr, H.W., 1967–76. Identification of a novel coronavirus in patients with severe acute respiratory syndrome. *N. Engl. J. Med.* 348 (20).
- FDA notifications, 2003. FDA approves Fuzeon, the first fusion inhibitor. *AIDS Alert* 18(6), 78–79.
- Gallagher, T.M., Buchmeier, M.J., 2001. Coronavirus spike proteins in viral entry and pathogenesis. *Virology* 279 (2), 371–374.

- Gallagher, W.R., 1987. Detection of a fusion peptide sequence in the transmembrane protein of human immunodeficiency virus. *Cell* 50 (3), 327–328.
- Gallagher, W.R., 1996. Similar structural models of the transmembrane proteins of Ebola and avian sarcoma viruses. *Cell* 85 (4), 477–478.
- Gallagher, W.R., Ball, J.M., Garry, R.F., Griffin, M.C., Montelaro, R.C., 1989. A general model for the transmembrane proteins of HIV and other retroviruses. *AIDS Res. Hum. Retroviruses* 5 (4), 431–440.
- Gallagher, W.R., Garry, R.F., 2003. Model of the pre-insertion region of the spike (S2) fusion glycoprotein of the human SARS coronavirus: implications for antiviral therapeutics.
- Gallagher, W.R., Segrest, J.P., Hunter, E., 1992. Are fusion peptides really “sided” insertional helices? *Cell* 70 (4), 531–532.
- Goldsmith, C.S., Tatti, K.M., Ksiazek, T.G., Rollin, P.E., Comer, J.A., Lee, W.W., Rota, P.A., Bankamp, B., Bellini, W.J., Zaki, S.R., 2004. Ultrastructural characterization of SARS coronavirus. *Emerg. Infect. Dis.* 10 (2), 320–326.
- Gorbalenya, A.E., Snijder, E.J., Spaan, W.J., 2004. Severe acute respiratory syndrome coronavirus phylogeny: toward consensus. *J. Virol.* 78 (15), 7863–7866.
- Holmes, K.V., 2005. Structural biology. Adaptation of SARS coronavirus to humans. *Science* 309 (5742), 1822–1823.
- Huang, I.C., Bosch, B.J., Li, F., Li, W., Lee, K.H., Ghiran, S., Vasilieva, N., Dermody, T.S., Harrison, S.C., Dormitzer, P.R., Farzan, M., Rottier, P.J., Choe, H., 2006. SARS coronavirus, but not human coronavirus NL63, utilizes Cathepsin L to infect ACE2-expressing cells. *J. Biol. Chem.* 281 (6), 3198–3203.
- Jayasinghe, S., Hristova, K., White, S.H., 2001. Energetics, stability, and prediction of transmembrane helices. *J. Mol. Biol.* 312 (5), 927–934.
- Jeffers, S.A., Tusell, S.M., Gillim-Ross, L., Hemmila, E.M., Achenbach, J.E., Babcock, G.J., Thomas Jr., W.D., Thackray, L.B., Young, M.D., Mason, R.J., Ambrosino, D.M., Wentworth, D.E., Demartini, J.C., Holmes, K.V., 2004. CD209L (L-SIGN) is a receptor for severe acute respiratory syndrome coronavirus. *Proc. Natl. Acad. Sci. U.S.A.* 101 (44), 15748–15753.
- Kilby, J.M., Hopkins, S., Venetta, T.M., DiMassimo, B., Cloud, G.A., Lee, J.Y., Alldredge, L., Hunter, E., Lambert, D., Bolognesi, D., Matthews, T., Johnson, M.R., Nowak, M.A., Shaw, G.M., Saag, M.S., 1998. Potent suppression of HIV-1 replication in humans by T-20, a peptide inhibitor of gp41-mediated virus entry. *Nat. Med.* 4 (11), 1302–1307.
- Kliger, Y., Levanon, E.Y., 2003. Cloaked similarity between HIV-1 and SARS-CoV suggests an anti-SARS strategy. *BMC Microbiol.* 3 (1), 20.
- Ksiazek, T.G., Erdman, D., Goldsmith, C.S., Zaki, S.R., Peret, T., Emery, S., Tong, S., Urbani, C., Comer, J.A., Lim, W., Rollin, P.E., Dowell, S.F., Ling, A.E., Humphrey, C.D., Shieh, W.J., Guarner, J., Paddock, C.D., Rota, P., Fields, B., DeRisi, J., Yang, J.Y., Cox, N., Hughes, J.M., LeDuc, J.W., Bellini, W.J., Anderson, L.J., 2003. A novel coronavirus associated with severe acute respiratory syndrome. *N. Engl. J. Med.* 348 (20), 1953–1966.
- Lai, M.M.C., Holmes, K.V., 2001. *Coronaviridae*: the viruses and their replication. In: Knipe, D.M., Howley, P.M. (Eds.), *Fundamental Virology*, fourth ed. Lippincott Williams & Wilkins, Philadelphia.
- Lalezari, J.P., Eron, J.J., Carlson, M., Cohen, C., DeJesus, E., Arduino, R.C., Gallant, J.E., Volberding, P., Murphy, R.L., Valentine, F., Nelson, E.L., Sista, P.R., Dusek, A., Kilby, J.M., 2003a. A phase II clinical study of the long-term safety and antiviral activity of enfuvirtide-based antiretroviral therapy. *AIDS* 17 (5), 691–698.
- Lalezari, J.P., Patel, I.H., Zhang, X., Dorr, A., Hawker, N., Siddique, Z., Kolis, S.J., Kinchelov, T., 2003b. Influence of subcutaneous injection site on the steady-state pharmacokinetics of enfuvirtide (T-20) in HIV-1-infected patients. *J. Clin. Virol.* 28 (2), 217–222.
- Lambert, D.M., Barney, S., Lambert, A.L., Guthrie, K., Medinas, R., Davis, D.E., Bucy, T., Erickson, J., Merutka, G., Petteway Jr., S.R., 1996. Peptides from conserved regions of paramyxovirus fusion (F) proteins are potent inhibitors of viral fusion. *Proc. Natl. Acad. Sci. U.S.A.* 93 (5), 2186–2191.
- Li, F., Li, W., Farzan, M., Harrison, S.C., 2005. Structure of SARS coronavirus spike receptor-binding domain complexed with receptor. *Science* 309 (5742), 1864–1868.
- Li, W., Moore, M.J., Vasilieva, N., Sui, J., Wong, S.K., Berne, M.A., Sundaraman, M., Sullivan, J.L., Luzuriaga, K., Greenough, T.C., Choe, H., Farzan, M., 2003. Angiotensin-converting enzyme 2 is a functional receptor for the SARS coronavirus. *Nature* 426 (6965), 450–454.
- Liu, S., Xiao, G., Chen, Y., He, Y., Niu, J., Escalante, C.R., Xiong, H., Farmer, J., Debnath, A.K., Tien, P., Jiang, S., Goldsmith, C.S., Tatti, K.M., Ksiazek, T.G., Rollin, P.E., Comer, J.A., Lee, W.W., Rota, P.A., Bankamp, B., Bellini, W.J., Zaki, S.R., 2004. Interaction between heptad repeat 1 and 2 regions in spike protein of SARS-associated coronavirus: implications for virus fusogenic mechanism and identification of fusion inhibitors. *Lancet* 363 (9413), 938–947.
- Luytjes, W., Sturman, L.S., Bredenbeek, P.J., Charite, J., van der Zeijst, B.A., Horzinek, M.C., Spaan, W.J., 1987. Primary structure of the glycoprotein E2 of coronavirus MHV-A59 and identification of the trypsin cleavage site. *Virology* 161 (2), 479–487.
- Magiorkinis, G., Magiorkinis, E., Paraskevis, D., Vandamme, A.M., Van Ranst, M., Moulton, V., Hatzakis, A., 2004. Phylogenetic analysis of the full-length SARS-CoV sequences: evidence for phylogenetic discordance in three genomic regions. *J. Med. Virol.* 74 (3), 369–372.
- Molloy, S.S., Bresnahan, P.A., Leppla, S.H., Klimpel, K.R., Thomas, G., 1992. Human furin is a calcium-dependent serine endoprotease that recognizes the sequence Arg-X-X-Arg and efficiently cleaves anthrax toxin protective antigen. *J. Biol. Chem.* 267 (23), 16396–16402.
- Owens, R.J., Tanner, C.C., Mulligan, M.J., Srinivas, R.V., Compans, R.W., 1990. Oligopeptide inhibitors of HIV-induced syncytium formation. *AIDS Res Hum Retroviruses* 6 (11), 1289–1296.
- Peiris, J.S., Lai, S.T., Poon, L.L., Guan, Y., Yam, L.Y., Lim, W., Nicholls, J., Yee, W.K., Yan, W.W., Cheung, M.T., Cheng, V.C., Chan, K.H., Tsang, D.N., Yung, R.W., Ng, T.K., Yuen, K.Y., 2003a. Coronavirus as a possible cause of severe acute respiratory syndrome. *Lancet* 361 (9366), 1319–1325.
- Peiris, J.S., Yuen, K.Y., Osterhaus, A.D., Stohr, K., 2003b. The severe acute respiratory syndrome. *N. Engl. J. Med.* 349 (25), 2431–2441.
- Qureshi, N.M., Coy, D.H., Garry, R.F., Henderson, L.A., 1990. Characterization of a putative cellular receptor for HIV-1 transmembrane glycoprotein using synthetic peptides. *AIDS* 4 (6), 553–558.
- Richardson, C.D., Scheid, A., Choppin, P.W., 1980. Specific inhibition of paramyxovirus and myxovirus replication by oligopeptides with amino acid sequences similar to those at the N-termini of the F1 or HA2 viral polypeptides. *Virology* 105 (1), 205–222.
- Rota, P.A., Oberste, M.S., Monroe, S.S., Nix, W.A., Campagnoli, R., Icenogle, J.P., Penaranda, S., Bankamp, B., Maher, K., Chen, M.H., Tong, S., Tamin, A., Lowe, L., Frace, M., DeRisi, J.L., Chen, Q., Wang, D., Erdman, D.D., Peret, T.C., Burns, C., Ksiazek, T.G., Rollin, P.E., Sanchez, A., Liffick, S., Holloway, B., Limor, J., McCaustland, K., Olsen-Rasmussen, M., Fouchier, R., Gunther, S., Osterhaus, A.D., Drosten, C., Pallansch, M.A., Anderson, L.J., Bellini, W.J., 2003. Characterization of a novel coronavirus associated with severe acute respiratory syndrome. *Science* 300 (5624), 1394–1399.
- Sainz Jr., B., Rausch, J.M., Gallagher, W.R., Garry, R.F., Wimley, W.C., 2005a. The aromatic domain of the coronavirus class I viral fusion protein induces membrane permeabilization: putative role during viral entry. *Biochemistry* 44, 947–958.
- Sainz Jr., B., Rausch, J.M., Gallagher, W.R., Garry, R.F., Wimley, W.C., 2005b. Identification and characterization of the putative fusion peptide of the severe acute respiratory syndrome-associated coronavirus (SARS-CoV) spike protein. *J. Virol.* 79 (11), 7195–7206.
- Sia, S.K., Carr, P.A., Cochran, A.G., Malashkevich, V.N., Kim, P.S., 2002. Short constrained peptides that inhibit HIV-1 entry. *Proc. Natl. Acad. Sci. U.S.A.* 99 (23), 14664–14669.
- Siddell, S.G., 1995. *Coronaviridae*; an Introduction. Plenum Press, New York, NY.
- Silburn, K.A., McPhee, D.A., Maerz, A.L., Pountourios, P., Whittaker, R.G., Kirkpatrick, A., Reilly, W.G., Mantley, M.K., Curtin, C.C., 1998. Efficacy of fusion peptide homologs in blocking cell lysis and HIV-induced fusion. *AIDS Res Hum Retroviruses* 14 (5), 385–392.
- Simmons, G., Reeves, J.D., Rennekamp, A.J., Amberg, S.M., Piefer, A.J., Bates, P., 2004. Characterization of severe acute respiratory syndrome-

- associated coronavirus (SARS-CoV) spike glycoprotein-mediated viral entry. *Proc. Natl. Acad. Sci. U.S.A.* 101 (12).
- Song, H.D., Tu, C.C., Zhang, G.W., Wang, S.Y., Zheng, K., Lei, L.C., Chen, Q.X., Gao, Y.W., Zhou, H.Q., Xiang, H., Zheng, H.J., Chern, S.W., Cheng, F., Pan, C.M., Xuan, H., Chen, S.J., Luo, H.M., Zhou, D.H., Liu, Y.F., He, J.F., Qin, P.Z., Li, L.H., Ren, Y.Q., Liang, W.J., Yu, Y.D., Anderson, L., Wang, M., Xu, R.H., Wu, X.W., Zheng, H.Y., Chen, J.D., Liang, G., Gao, Y., Liao, M., Fang, L., Jiang, L.Y., Li, H., Chen, F., Di, B., He, L.J., Lin, J.Y., Tong, S., Kong, X., Du, L., Hao, P., Tang, H., Bernini, A., Yu, X.J., Spiga, O., Guo, Z.M., Pan, H.Y., He, W.Z., Manuguerra, J.C., Fontanet, A., Danchin, A., Niccolai, N., Li, Y.X., Wu, C.I., Zhao, G.P., 2005. Cross-host evolution of severe acute respiratory syndrome coronavirus in palm civet and human. *Proc. Natl. Acad. Sci. U.S.A.* 102 (7), 2430–2435.
- Taguchi, F., 1995. The S2 subunit of the murine coronavirus spike protein is not involved in receptor binding. *J. Virol.* 69 (11), 7260–7263.
- Taguchi, F., Shimazaki, Y.K., 2000. Functional analysis of an epitope in the S2 subunit of the murine coronavirus spike protein: involvement in fusion activity. *J. Gen. Virol.* 81 (Pt 12), 2867–2871.
- Tripet, B., Howard, M.W., Jobling, M., Holmes, R.K., Holmes, K.V., Hodges, R.S., 2004. Structural characterization of the SARS-coronavirus spike S fusion protein core. *J. Biol. Chem.* 279 (20), 20836–20849.
- Wang, P., Chen, J., Zheng, A., Nie, Y., Shi, X., Wang, W., Wang, G., Luo, M., Liu, H., Tan, L., Song, X., Wang, Z., Yin, X., Qu, X., Wang, X., Qing, T., Ding, M., Deng, H., 2004. Expression cloning of functional receptor used by SARS coronavirus. *Biochem. Biophys. Res. Commun.* 315 (2), 439–444.
- Watanabe, S., Takada, A., Watanabe, T., Ito, H., Kida, H., Kawaoka, Y., 2000. Functional importance of the coiled-coil of the Ebola virus glycoprotein. *J. Virol.* 74 (21), 10194–10201.
- White, S.H., Wimley, W.C., 1999. Membrane protein folding and stability: physical principles. *Annu. Rev. Biophys. Biomol. Struct.* 28, 319–365.
- Wild, C., Greenwell, T., Matthews, T., 1993. A synthetic peptide from HIV-1 gp41 is a potent inhibitor of virus-mediated cell–cell fusion. *AIDS Res. Hum. Retroviruses* 9 (11), 1051–1053.
- Wild, C., Oas, T., McDanal, C., Bolognesi, D., Matthews, T., 1992. A synthetic peptide inhibitor of human immunodeficiency virus replication: correlation between solution structure and viral inhibition. *Proc. Natl. Acad. Sci. U.S.A.* 89 (21), 10537–10541.
- Wimley, W.C., White, S.H., 1996. Experimentally determined hydrophobicity scale for proteins at membrane interfaces. *Nat. Struct. Biol.* 3 (10), 842–848.
- Wong, S.K., Li, W., Moore, M.J., Choe, H., Farzan, M., 2004. A 193-amino acid fragment of the SARS coronavirus S protein efficiently binds angiotensin-converting enzyme 2. *J. Biol. Chem.* 279 (5), 3197–3201.
- Wu, X.D., Shang, B., Yang, R.F., Yu, H., Ma, Z.H., Shen, X., Ji, Y.Y., Lin, Y., Wu, Y.D., Lin, G.M., Tian, L., Gan, X.Q., Yang, S., Jiang, W.H., Dai, E.H., Wang, X.Y., Jiang, H.L., Xie, Y.H., Zhu, X.L., Pei, G., Li, L., Wu, J.R., Sun, B., 2004. The spike protein of severe acute respiratory syndrome (SARS) is cleaved in virus infected Vero-E6 cells. *Cell Res.* 14 (5), 400–406.
- Xu, Y., Liu, Y., Lou, Z., Qin, L., Li, X., Bai, Z., Pang, H., Tien, P., Gao, G.F., Rao, Z., 2004a. Structural basis for coronavirus-mediated membrane fusion. Crystal structure of mouse hepatitis virus spike protein fusion core. *J. Biol. Chem.* 279 (29), 30514–30522.
- Xu, Y., Lou, Z., Liu, Y., Pang, H., Tien, P., Gao, G.F., Rao, Z., 2004b. Crystal structure of SARS-CoV spike protein fusion core. *J. Biol. Chem.* 1 (1), 1.
- Xu, Y., Zhu, J., Liu, Y., Lou, Z., Yuan, F., Cole, D.K., Ni, L., Su, N., Qin, L., Li, X., Bai, Z., Bell, J.I., Pang, H., Tien, P., Gao, G.F., Rao, Z., 2004c. Characterization of the Heptad Repeat Regions, HR1 and HR2, and design of a fusion core structure model of the spike protein from severe acute respiratory syndrome (SARS) coronavirus. *Biochemistry* 43 (44), 14064–14071.
- York, J., Nunberg, J.H., 2004. Role of hydrophobic residues in the central ectodomain of gp41 in maintaining the association between human immunodeficiency virus type 1 envelope glycoprotein subunits gp120 and gp41. *J. Virol.* 78 (9), 4921–4926.
- Young, J.K., Li, D., Abramowitz, M.C., Morrison, T.G., 1999. Interaction of peptides with sequences from the Newcastle disease virus fusion protein heptad repeat regions. *J. Virol.* 73 (7), 5945–5956.
- Yuan, K., Yi, L., Chen, J., Qu, X., Qing, T., Rao, X., Jiang, P., Hu, J., Xiong, Z., Nie, Y., Shi, X., Wang, W., Ling, C., Yin, X., Fan, K., Lai, L., Ding, M., Deng, H., 2004. Suppression of SARS-CoV entry by peptides corresponding to heptad regions on spike glycoprotein. *Biochem. Biophys. Res. Commun.* 319 (3), 746–752.
- Zhu, J., Xiao, G., Xu, Y., Yuan, F., Zheng, C., Liu, Y., Yan, H., Cole, D.K., Bell, J.I., Rao, Z., Tien, P., Gao, G.F., 2004. Following the rule: formation of the 6-helix bundle of the fusion core from severe acute respiratory syndrome coronavirus spike protein and identification of potent peptide inhibitors. *Biochem. Biophys. Res. Commun.* 319 (1), 283–288.